

3D PRINTED ORTHOPAEDIC FUSION WITH LATERAL APPROACH THROUGH THE INTERVERTEBRAL SPACE FOR LUMBAR LORDOSIS

WEI CHENG, TIANMING GUO*, JIANPING GUO, QUANXIANG LIU

Orthopaedic second treatment area, Affiliated Hospital of Beihua University, Jilin, Jilin132000, China

ABSTRACT

Objective: The feasibility and safety of adding a lateral integrated 3 D printing fusion device in a laterolateral lumbar intervertebral fusion procedure (oblique lateral interbody fusion, OLIF) were analyzed.

Methods: 11 patients 2019 were treated with lumbar convex deformity from February 2019 to February 2021. Operation time, intraoperative bleeding, intraoperative and postoperative complications were recorded; compare 1 week postoperative, visual analogue scale (VAS) 3 months and last follow-up, Oswestry disability index (ODI), the MOS item short form health survey (SF-36); preoperative, 1 week, and 3 months postoperative lumbar lordosis (LL), fused segment lordosis (FSL), sagittal vertical axis (SVA), pelvic incidence (PI), pelvic tilt (PT), sacral slope (SS), Disc height (DH). CT observed the fusion segment fusion rate at 6 months post-surgery.

Results: The average operation time of 11 patients was (187.18±39.29) min, and the mean intraoperative bleeding was (64.45±31.19) ml. Low back pain VAS score, ODI, SF-36 decreased from preoperative score (7.37±1.02), 58.92±11.45, (53.82±12.44) to (0.64±0.49), 11.86±5.25, (77.45±8.97), all statistically significant ($P<0.05$). Patients were statistically significant in LL, FSL, SVA, PI, PT, SS, DH 3 months after surgery compared to preoperative comparison ($P<0.05$). SVA and PT were significantly decreased 3 months after operation, with statistical significance ($P<0.05$). There was no significant change in PI 3 months after surgery compared with that before surgery ($P>0.05$). No displacement and sinking complications occurred in the flanking integrated 3 D printed vertebral fusion device at 6 months after surgery. No serious complications such as neurological and vascular injury were observed after surgery.

Conclusion: For patients with lumbar kyphosis, the treatment of flanking integrated 3D printing fusion device has satisfactory clinical effect. It has developed a more minimally invasive way and choice for the treatment of lumbar kyphosis.

Keywords: Three-dimensional printing cage, oblique lateral interbody fusion, kyphosis, correction, orthopedic.

DOI: 10.19193/0393-6384_2022_5_522

Received March 15, 2022; Accepted June 20, 2022

Introduction

With the rapid increase in population aging, lumbar kyphosis is the most harmful and fastest growing degenerative disease of the lumbar spine as well as a common type of spinal deformity⁽¹⁾. Its causes mainly include, lumbar degenerative disease, osteoporotic vertebral compression fracture (OVCF), old lumbar fracture, and mandatory spondylolisthesis⁽²⁻³⁾. Among them, lumbar degenerative kyphosis is the most common with

far greater harm than degenerative scoliosis. Early lumbar kyphosis leads to increased muscle and fascia tension in the patient's low back, and local inflammatory response, biomechanical changes in the spine, with patients experiencing low back pain⁽⁴⁾. The persistent pain symptoms prompt the patient to often maintain an anterior tilt of the trunk, which subsequently aggravates the lumbar kyphosis⁽⁵⁾. Severe lumbar kyphosis leads to lumbar spinal stenosis of the corresponding segment, spinal cord compression and thus neurological symptoms,

resulting in a severe decrease in the patient's quality of life⁽⁵⁾. Severe lumbar kyphosis is often treated clinically with orthopedic surgery. Some common surgical procedures include Smith-Petersen osteotomy (SPO), pedicle subtraction osteotomy (PSO), Ponte osteotomy, vertebral column resection (VCR), etc.⁽⁶⁻⁹⁾. However, posterior osteotomy orthopedic surgery still has risks associated with long operative time, high bleeding and complications⁽¹⁰⁻¹¹⁾. Due to the development of the lateral anterior approach to the lumbar spine in recent years, some scholars have achieved satisfactory clinical results in the treatment of lumbar lordosis by subtotal laminectomy and fusion with the lateral anterior approach.

Its advantages include reduced surgical trauma, decreased operative time and risk of intraoperative spinal cord nerve injury, but there is still a large amount of bleeding from the lateral side of the vertebral body during lateral subtotal resection⁽¹²⁾. How to reduce surgical trauma and perform minimally invasive surgery has become a hot and difficult issue in spinal orthopedic surgery. Our department has independently developed 3D printed orthopedic fusion since 2019 to treat lumbar lordosis by implanting large angle fusion in the intervertebral space through lateral lumbar interbody fusion (LLIF) technology. The preliminary efficacy, safety and feasibility are reported below.

Materials and methods

Inclusion and exclusion criteria

Inclusion criteria:

- Old lumbar fracture with kyphosis;
- Thoracolumbar wedge-shaped kyphosis and degenerative multivertebral kyphosis;
- Lumbar kyphosis $\geq 40^\circ$;
- Persistent low back pain not relieved by conservative treatment, and the duration of the disease is greater than 6 months.

Exclusion criteria:

- Combined spinal infection or spinal tumor;
- Fresh fracture confirmed by MRI T2 lipopressor image;
- Vertebral bone density check T value ≤ -2.5 SD;
- Primary osteoporosis (senile osteoporosis, idiopathic osteoporosis, postmenopausal osteoporosis), secondary osteoporosis (hyperthyroidism, hyperparathyroidism, diabetes mellitus);
- Concomitant severe organic pathology that cannot tolerate surgery;

- Preoperative lumbar spine CT showing fusion of the articular eminence;
- Old fracture causing angular kyphosis;
- Presence of neurological symptoms in the lower extremities;
- Case lost to follow-up.

General data

A total of 11 cases were included in this group. The general data of the patients is detailed in Table 1.

Indicator	Data
Age (years)	67.43±9.21
Sex (male/female)	3/8
Low back pain (cases)	11
Neurological impairment (cases)	2
Parietal spine (cases, L1/L2/L3)	2/3/6
Bone density (T value)	-1.14±0.98
Fusion of segments (cases, 2/3)	7/4

Table 1: Basic information of the patient.

3D printed orthopaedic fusion design solution

Some studies have shown that the application of a large anterior convexity angle (20° - 30°) interbody fusion with release of the anterior longitudinal ligament in the lateral approach can correct the lumbar anterior convexity angle to some extent⁽¹³⁻¹⁴⁾. In this study, a large number of cases of lumbar kyphosis were collected and the lumbar peri-axial imaging parameters were obtained by CT scanning of the lumbar spine. Intraoperative correction of lumbar lordosis angle and intervertebral space height was simulated by 3D modeling. Statistical analysis was performed based on the morphology of the adjacent upper and lower endplates. Accordingly, a 3D printed orthopedic fusion (made of titanium microporous metal) with a 20° anterior convexity angle was designed. The anterior height of the fusion was 13 mm, 14 mm, and 15 mm, respectively. The length of the fusion was 45 mm and the width was 20 mm (Figure 1).

After general anesthesia took effect, the patient was placed in the right lateral position, and the LLIF surgical incision was made in the left lumbar region. An incision of approximately 8 cm in length was made on the anterolateral side of the lateral fluoroscopic projection with the parietal vertebral body as the center. The skin was incised and the external oblique abdominal muscle, internal oblique abdominal muscle and transverse abdominal muscle were separated. The T1-L1 and L1-2 gaps were mostly obscured by the ribs. The distal ribs of thorax

11 needed to be freed and resected about 3.0 cm in length. The posterior peritoneal space was separated to reach the anterior space of the psoas major muscle. The psoas major muscle was pulled to the dorsal side, exposed, and positioned with C-arm fluoroscopy. We selected two or three intervertebral spaces in the convex apex vertebral region, cut the fibrous rings of the corresponding intervertebral segments with a sharp knife, removed the 2.0 cm wide nucleus pulposus and disc tissue in the central region of the vertebral body with a nucleus pulposus forceps and a square scraper, excised the contralateral fibrous ring, scraped to the upper and lower endplates, implanted a conventional trial mold, and gradually propped up the intervertebral space. At the same time, we observed the degree of tension of the anterior longitudinal ligament, inserted the brain pressure plate to protect the anterior tissue of the vertebral body, partially cut the anterior longitudinal ligament, and then gradually opened the vertebral space, and repeated the above operations until we placed the 20° fusion trial mold.

A custom 3D printed orthopedic fusion was implanted in each of the three intervertebral spaces. On C-arm fluoroscopy, the fusion was well positioned with good correction of the posterior deformity angle. The dorsal convex vertebral region was pushed with force to further increase the anterior convexity, and the lateral screws were drilled and locked. The patient's position was changed to prone, the lumbar back area was disinfected, sterile towel sheets were placed, and percutaneous pedicle screw fixation was performed.

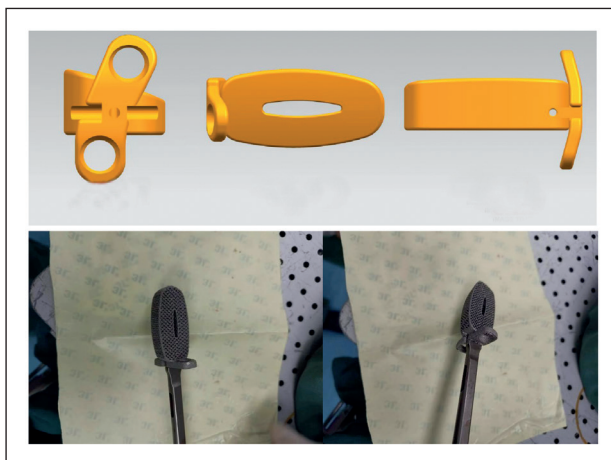


Figure 1: Schematic diagram of the flanking integrated 3D printing cage.

Surgical method

After general anesthesia took effect, the patient was placed in the right lateral position, and the

LLIF surgical incision was made in the left lumbar region. An incision of approximately 8 cm in length was made on the anterolateral side of the lateral fluoroscopic projection with the parietal vertebral body as the center.

The skin was incised and the external oblique abdominal muscle, internal oblique abdominal muscle and transverse abdominal muscle were separated. The T1-L1 and L1-2 gaps were mostly obscured by the ribs. The distal ribs of thorax 11 needed to be freed and resected about 3.0 cm in length. The posterior peritoneal space was separated to reach the anterior space of the psoas major muscle. The psoas major muscle was pulled to the dorsal side, exposed, and positioned with C-arm fluoroscopy. We selected two or three intervertebral spaces in the convex apex vertebral region, cut the fibrous rings of the corresponding intervertebral segments with a sharp knife, removed the 2.0 cm wide nucleus pulposus and disc tissue in the central region of the vertebral body with a nucleus pulposus forceps and a square scraper, excised the contralateral fibrous ring, scraped to the upper and lower endplates, implanted a conventional trial mold, and gradually propped up the intervertebral space.

At the same time, we observed the degree of tension of the anterior longitudinal ligament, inserted the brain pressure plate to protect the anterior tissue of the vertebral body, partially cut the anterior longitudinal ligament, and then gradually opened the vertebral space, and repeated the above operations until we placed the 20° fusion trial mold. A custom 3D printed orthopedic fusion was implanted in each of the three intervertebral spaces. On C-arm fluoroscopy, the fusion was well positioned with good correction of the posterior deformity angle. The dorsal convex vertebral region was pushed with force to further increase the anterior convexity, and the lateral screws were drilled and locked.

The patient's position was changed to prone, the lumbar back area was disinfected, sterile towel sheets were placed, and percutaneous pedicle screw fixation was performed.

Postoperative management

Postoperatively, antibiotics were administered for 1 day to prevent infection. The patient sat up under the protection of a lumbar bib for 3 days after surgery, and gradually started to walk out of bed for exercise. Postoperative follow-up was performed regularly to review the frontal and lateral radiographs of the lumbar spine and the full-length frontal and

lateral radiographs of the spine. The lumbar spine CT was reviewed 6 months after surgery to observe the fusion of the lumbar spine.

Evaluation criteria

Clinical outcome evaluation included operative time, intraoperative bleeding, intraoperative and postoperative complications (end-plate injury, end-plate collapse, fusion sink ≥ 2 mm, hemopneumothorax, nerve injury, cerebrospinal fluid leak, etc.), visual analogue scale (VAS) for preoperative, 1 week postoperative, 3 months postoperative and final follow-up pain, Oswestry dysfunction index (ODI), and the MOS item short form health survey (SF-36).

The imaging evaluation included radiographic measurements of lumbar lordosis (LL), fused segment lordosis (FSL), sagittal vertical axis (SVA), pelvic incidence (PI), pelvic tilt (PT), sacral slope (SS), and disc height (DH) before surgery, 1 week after surgery, and 3 months after surgery. The fusion rate of fused segments was observed by CT at 6 months postoperatively.

Measurement methods

- LL: The angle between the L1 terminal superior plate and the L5 vertebral body inferior terminal plate extension line in a lateral X-ray.

- FSL: The angle between the upper endplate of the proximal fused vertebra and the upper endplate of the distal fused vertebra on a lateral lumbar X-ray.

- SVA: The distance between C7pl and the upper rear corner of S1.

- PI: Make a vertical line through the midpoint of S1 upper endplate. The angle between this vertical line and the line connecting the center of the femoral head.

- PT: The angle between the midpoint of the S1 endplate and the line connecting the center of the femoral head and the vertical plumb line.

- SS: The angle between the end plate and the horizontal line on S1.

- DH: Anterior intervertebral space height + posterior intervertebral space height/2.

Statistical method

SPSS 26.0 software was applied to analyze the above data statistically. The measurement data conforming to normal distribution were expressed as ($\bar{x} \pm s$). The indicators were tested by one-way ANOVA test at different time before and after surgery.

Results

Perioperative situation

All 11 patients completed the surgery successfully. The operative time ranged from 135 to 262 min, with a mean of (187.18 \pm 39.29) min. The intraoperative bleeding volume ranged from 30 to 150 ml, with a mean of (64.45 \pm 31.19) ml. All patients were followed up for more than 6 months, with a mean follow-up time of (8.36 \pm 2.34) months.

One patient had intraoperative segmental vascular injury, which was filled with gelatin sponge and stopped by gauze pressure, without active bleeding after surgery. One patient had peritoneal injury, which was tightly sutured during surgery, without complications at 8 months postoperative follow-up. Postoperatively, two patients developed abdominal distension, which was relieved after symptomatic treatment was given (Table 2).

	Complications	Number of cases
Intraoperative complications	Endplate injury	0
	Hemopneumothorax	0
	Nerve root injury	0
	Segmental Vascular Injury	1
	Iliac vessel injury	0
	Peritoneal injury	1
	Ureteral injury	0
Postoperative complications	Infection	0
	Loosening of the fusion (displacement, sinking)	0
	Genital femoral nerve symptoms	0
	Intestinal symptoms	2
	Abnormal lower extremity movement or sensation	0

Table 2: Intraoperative and postoperative complications.

Clinical efficacy evaluation

Patients' VAS, ODI, and SF-36 improved significantly at 1 week, 3 months, and at the final follow-up after surgery compared with the preoperative period, with statistically significant differences ($P < 0.05$) (Table 3).

	Preoperative	1 week postoperative	3 months postoperative	Final Follow-up	F-value	P-value
VAS	7.37 \pm 1.02	2.36 \pm 0.51	1.36 \pm 1.02	0.64 \pm 0.49	151.50	0.00
ODI	58.92 \pm 11.45	15.45 \pm 5.59	13.31 \pm 4.97	11.86 \pm 5.25	102.79	0.00
SF-36	53.82 \pm 12.44	78.18 \pm 10.27	79.18 \pm 10.06	77.45 \pm 8.97	14.60	0.00

Table 3: The comparison of VAS, ODI, and SF-36 between preoperative, 1 week after operation and 3 months after operation.

Imaging evaluation

The LL, FSL, SS, and DH were significantly higher in patients one week and 3 months postoperatively compared with preoperatively, and the difference was statistically significant ($P<0.05$). The SVA and PT were significantly reduced one week and 3 months after surgery compared with those before surgery, and the difference was statistically significant ($P<0.05$). The PI and DH did not change significantly at one week and 3 months postoperatively compared with preoperatively, without statistically significant differences ($P>0.05$) (Table 4).

	Preoperative	1 week postoperative	3 months postoperative	F-value	P-value
LL (°)	29.18±3.76	45.18±3.60	43.00±1.30	54.093	0.00
FSL (°)	-53.45±2.94	4.27±2.37	4.18±2.17	1881.266	0.00
SVA (cm)	4.75±0.70	3.20±0.49	3.15±0.45	20.208	0.00
PI (°)	47.36±3.80	48.09±2.66	48.64±4.65	0.311	0.74
PT (°)	32.09±2.02	19.73±1.74	19.91±2.21	138.091	0.00
SS (°)	14.73±2.57	28.64±2.20	28.44±2.45	116.515	0.00
DH (°)	8.77±1.05	11.26±1.07	11.22±1.35	48.402	0.00

Table 4: Results of imaging evaluation indicators at different time.

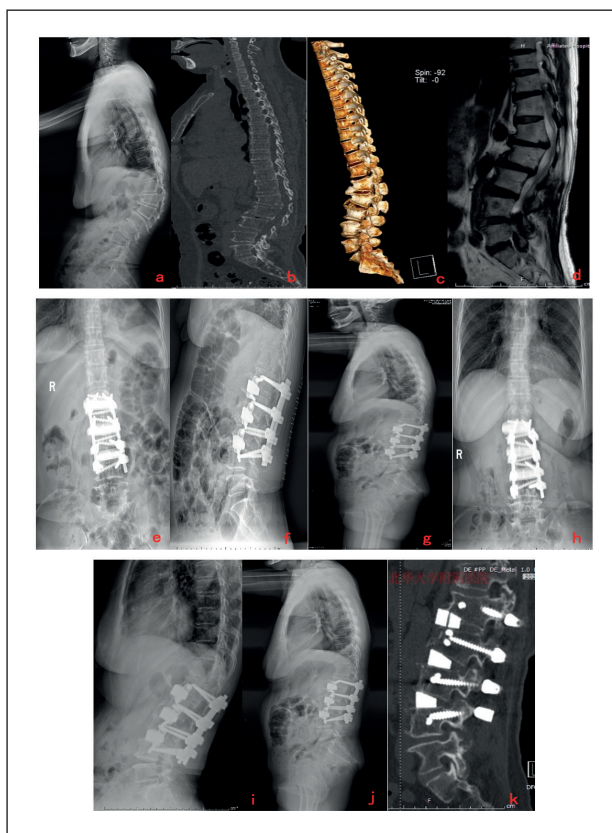


Figure 2: The patient, female, 59 years old, L1 and L2 vertebral wedges, lumbar compression fracture, deformity. Applied a lateral translateral approach lumbar

fusion combined with posterior percutaneous pedicle screw fixation to correct lumbar kyphosis deformity. a: full-length X-ray of the spine shows wedge change of L1 spine; b, c: Flat CT scan and 3 D reconstruction of the lumbar spine. The vertebral region is located in the L1 vertebra, L1, L2 vertebral wedge change, L1~2 vertebral space narrowing; d: lumbar magnetic resonance shows lumbar kyphosis deformity, L1, L2 vertebral wedge change, L1~2 Sinal narrowing; X-ray and X-ray of the lumbar spine were reviewed 1 week after ; e, f, g: The ateral tablets showed postoperative lumbar kyphosis correction, Lumbar sagittal balance was recovered after surgery; h, i: Review of X-ray in the lateral lumbar spine 6 months after surgery showed osteophyte absorption of the anterior margin of L 1 to 2 vertebral space, The 3D printed prosthesis has no collapse, displacement, or loosening;j: Full-length X-ray of lumbar spine review 6 months after the operation showed that the lumbar anterior convex was good; k: lumbar C T 6 months after the operation, see 3D printing fusion interface seamless and the upper and lower end plate, closely connected, bone fusion signs, good fusion position, no loosening and vertebral space collapse, showing exact fixation.

Discussion

Imbalance in the sagittal plane of the spine in patients with lumbar kyphosis is a major cause of low back pain. Long-term lumbar kyphosis results in increased paravertebral muscle tone and aggravates the degeneration of adjacent segments. Therefore, it is crucial to restore the sagittal balance of the spine in the treatment of lumbar kyphosis. Currently, the common orthopedic surgery is mainly posterior orthopedic osteotomy, but the posterior surgery requires stripping the paravertebral muscles and destroying the posterior spinal column system, which results in heavy bleeding, high risk and many complications. In recent years, domestic and international literature has reported the excellent results of lateral surgery in the treatment of lumbar spondylolisthesis, lumbar spinal stenosis, and lumbar sagittal and coronal imbalance.

Most scholars believe that lateral spinal sagittal and coronal imbalance surgery has obvious technical advantages over posterior surgery. The main point of the LLIF technique is to reach the lateral side of the intervertebral space through the posterior peritoneal space and implant a large fusion on the lateral side of the intervertebral space, thus restoring the height of the intervertebral space and the original physiological curvature of the spine. The natural human gap approach, operating in the bloodless vertebral space, has the minimally invasive features of less bleeding,

less trauma and shorter operation time compared to the traditional posterior approach. The large fusion also has technical advantages in correcting sagittal and coronal imbalances of the spine. Min-soo Cho concluded from an imaging analysis of patients undergoing lateral versus posterior lumbar surgery that the lateral fusion procedure was significantly superior to the posterior procedure in correcting sagittal imbalances.

The main reasons for this were the larger and more stable lateral fusion and the presence of an anterior convexity of the fusion itself, which was closer to the normal anatomy of the body⁽¹⁵⁾. However, for severe lumbar kyphosis, there are still significant limitations in the correction of sagittal imbalance by lateral interbody fusion orthopedics, which is due to the fact that the effect of lateral fusion on the correction of pronation depends mainly on the angle and position of the fusion device⁽¹⁶⁾. The existing lateral fusions generally have an anterior convexity angle of 8-12°⁽¹⁷⁾, which cannot achieve adequate correction. Based on the above considerations, we designed a 3D printed orthopedic fusion with an anterior convexity angle of 20°. The correction of the retroconvex deformity was achieved by multi-segmental spinal gap orthosis.

It has been reported in the literature that ALIF increases the correction of lumbar lordosis by an average of 2° compared to LLIF for the same segmental intervertebral fusion⁽¹⁸⁾. The main reason for this is that the anterior longitudinal ligament is severed during the ALIF procedure, weakening the anterior lumbar soft tissue tension⁽¹⁹⁾. In this study, a fusion with greater anterior convexity was implanted laterally to increase the height of the anterior half of the intervertebral space and anterior longitudinal ligament tension, with no or a slight increase in the height of the posterior portion of the intervertebral space and posterior longitudinal ligament. For orthopedic purposes, the height of the anterior half of the intervertebral space needed to be opened to prevent endplate injury during fusion placement. The relaxation of the anterior half of the intervertebral space and the partial severance of the anterior longitudinal ligament were necessary to reduce the pressure on the anterior part of the intervertebral space and to achieve adequate orthosis. In the upper lumbar portion of the posterior convex apex, the area of the intervertebral space was small and stressful. A fusion with a large anterior convexity angle would be less stable in the sagittal plane⁽¹⁶⁾. At the same time, the anterior longitudinal ligament was

partially severed and the anterior tension band was weakened, which further decreased the stability of the fusion device. In order to prevent the fusion from instability, displacement and loosening, we designed an integrated lateral wing to increase the stability of the fusion and prevent loosening and displacement through the fixation of the lateral wing screws.

The lumbar spine has a wedge shape due to lumbar kyphosis, as well as deformities in the adjacent upper and lower vertebral endplates. It is difficult to fit the upper and lower endplates with conventional PEEK intervertebral fusion devices⁽²⁰⁾. 3D printed as a porous structured titanium fusion device is similar to the elastic modulus of bone tissue. The pore structure of the fusion surface is similar to that of bone trabeculae, which facilitates bone ingrowth. The rough structure of its surface increases the interface friction and reduces the risk of fusion displacement⁽²¹⁾.

Meanwhile, the 3D printed fusion device can be customized to match the irregularity of the endplate defect morphology based on the preoperative 3D CT measurement of the endplate morphology to further individualize the treatment. Some studies have reported that the presence or absence of simultaneous posterior nail bar fixation during lateral surgery has an impact on lumbar sagittal parameters⁽²²⁾. Additional posterior fixation on top of placement of a lateral interbody fusion can add approximately 1-3° to the correction of anterior convexity⁽²³⁾. The reason for this is that the lumbar intervertebral space is anteriorly high and posteriorly low, while the intervertebral space of diseased vertebrae with posterior convex deformity is anteriorly low and posteriorly high. When the fusion is placed in the lateral approach, the anterior aspect of the intervertebral space is propped open, and at the same time, a gap appears between the upper and lower endplates and the fusion.

During fixation of the lateral screws, the skin in the spinous region of the posterior paracentral vertebra is pushed ventrally with bare hands to further improve the anterior convexity and to ameliorate the apposition of the posterior part of the fusion to the upper and lower endplates. The posterior nail bar fixation has a tension band fixation effect, using the posterior spinal column structure as a hinge to maintain the anterior lumbar lordosis while allowing further posterior apposition of the fusion to the upper and lower endplates. In this study, a large angle fusion was used, and in order to improve or maintain the posterior apposition of the fusion to the

upper and lower endplates, increase the corrective effect, and increase the stability and fixation strength of the fusion, we performed orthopedic surgery with additional percutaneous pedicle screw fixation.

Fusion settling in spinal interbody fusion is usually considered a normal process of endplate remodeling due to biomechanical loading during bone healing without substantial clinical implications⁽²⁴⁾. For OLIF surgery, excessive fusion settling (≥ 2 mm) can lead to decreased surgical indirect decompression, which can result in reduced foraminal height and cause neurological symptoms. To prevent the fusion from shifting or sinking in the distant postoperative period, the intraoperative placement of the 3D printed fusion should be centered. Placement of the fusion too far forward will result in too little correction of lumbar. The fusion that is too posterior will increase local endplate pressure and increase the risk of endplate collapse⁽²⁵⁾. The vertebral space should be propped open before implantation to prevent fusion impact damage to the endplate and secondary collapse⁽²⁶⁾. The degree of osteoporosis of the lumbar vertebral body should be assessed preoperatively, so this study excluded patients with a bone mineral density T value less than -2.5 from the exclusion criteria.

Traditional posterior osteotomies such as SPO, PSO, and Ponte require destruction of the posterior or three-column structures of the spine with resection of the articular eminence, the lamina, and even the vertebral body of the anterior middle column⁽²⁷⁾. Compared with the above posterior osteotomy, the LLIF approach to intervertebral space orthopedics, through the natural space to reach the intervertebral disc operation, bloodless state to perform surgery, without the operation of the three columns of the spine osteotomy, significantly reduce the amount of surgical bleeding. The literature has shown that the average bleeding volume of Ponte osteotomy is more than 700 ml, while the intraoperative bleeding volume in this study was only about 65 ml⁽²⁸⁾. In contrast, osteotomies such as SPO and PSO are more extensive and bleed more than Ponte osteotomy. Transforaminal orthopedic fusion with a 3D printed orthopedic fusion significantly reduces surgical bleeding and trauma compared to posterior conventional osteotomy orthopedic surgery.

At the same time, traditional osteotomy orthopedics require 8-10 segmental pedicle nail fixation because of the loss of stability due to disruption of the posterior spinal column or three-column structure. In connection with the

intervertebral disc, many researches⁽²⁹⁻³²⁾ have been done at the cellular and molecular levels, and researches are being carried out in this regard. In the future, it may be possible to connect the results of cellular and molecular research with 3D printed orthopaedic fusion. In this study, the stability of the segments was ensured by the good support of the fusion implanted in the anterior column of the spine and the integrity of the posterior column. The role of posterior nail bar fixation was limited to increasing fusion stability, apposition and three-dimensional strength. The number of posterior nail bar fixation segments was only 3-4, which significantly shortened the number of fixation segments compared to posterior osteotomy orthopedic surgery.

There are still some limitations of this study. The number of cases collected in this study was limited, and the error of statistical analysis was large. Also, the follow-up of long-term postoperative outcomes was insufficient. On the other hand, although we posteriorly squeezed the area around the parietal vertebrae during fixation of the lateral screws to increase the anterior lumbar convexity angle and to maximize the posterior attachment of the fusion to the upper and lower endplates behind the intervertebral space, the effect of posterior fixation to correct the anterior convexity was diminished by performing posterior pedicle screw surgery after fixation of the lateral screws. This study focused on the introduction of orthopedic cages and did not systematically analyze the orthopedic effect of posterior screw rods.

Conclusion

In conclusion, 3D-printed orthopedic fusion device for the treatment of lumbar kyphosis has good feasibility and safety.

The surgery is performed through a natural gap approach without destroying bony structures, with fewer fixed segments, less bleeding, and no serious complications, which has good application prospects and provides a minimally invasive idea for orthopaedic kyphosis.

References

- 1) Spiegl UJ, Fischer K, Schmidt J, et al. The conservative treatment of traumatic thoracolumbar vertebral fractures [J]. *Dtsch Arztebl Int*, 2018, 115(42): 697-704.
- 2) Sabou S, Lagaras A, Verma R, et al. Comparative study of multilevel posterior interbody fusion plus anterior longitudinal ligament release versus classic multilevel posterior interbody fusion in the treatment of adult spinal deformities [J]. *J Neurosurg Spine*, 2019, (1) 5: 1-7.
- 3) Bian Z, Gui Y, Feng F, et al. Comparison of anterior, posterior, and anterior combined with posterior surgical treatment of thoracic and lumbar spinal tuberculosis: a systematic review [J/OL]. *J Int Med Res*, 2019, DOI: 10.1177/0300060519830827.
- 4) Lazennec JY, Neves N, Rousseau MA, et al. Wedge osteotomy for treating post-traumatic kyphosis at thoracolumbar and lumbar levels [J]. *J Spinal Disord Tech*, 2006, 19(7): 487-494.
- 5) Roussouly P, Nnadi C. Sagittal plane deformity: an overview of interpretation and management [J]. *Eur Spine J*, 2011, 19(11): 1824-1836
- 6) Enercon M, Ozturk C, Kahraman S, et al. Osteotomies/spinal column resections in adult deformity [J]. *Eur Spine J*, 2013, 22(2): 254-264.
- 7) Sun X, Chen X, Chen ZF, et al. Ponte osteotomy combined with four-rod alternating compression orthopaedic technique for the treatment of kyphosis in Newman's disease [J]. *Chinese Journal of Orthopaedics*, 2017, 37(3): 129-136.
- 8) Yang XX, Fan TQ, Chen GH, et al. Research progress of osteotomy orthopedic surgery for posterior convex deformity in ankylosing spondylitis [J]. *Chinese Journal of Spinal Cord*, 2021, 31(04): 347-354.
- 9) Zhang HQ, Li M, Wang YX, et al. Minimum 5-year follow-up outcomes for comparison between titanium mesh cage and allogeneic bone graft to reconstruct anterior column through posterior approach for the surgical treatment of thoracolumbar spinal tuberculosis with kyphosis [J]. *World Neurosurg*, 2019, 19(19): 30817-30824.
- 10) Chen CH, Guo QG, Zhang HH. "PSO combined with SPO osteotomy versus multi-segment SPO osteotomy for traumatic thoracolumbar kyphosis." *Chinese Journal of Orthopaedic Surgery* 27.10 (2019): 895-900. DOI: CNKI:SUN:ZJXS.0.2019-10-010.
- 11) Wu XG, Li XB, Guo JB, et al. Combined PSO+SPO osteotomy for thoracolumbar kyphosis [J]. *Chinese Journal of Clinical Physicians (Electronic Edition)*, 2016, 10(03): 373-376.
- 12) Jiang Y, GUO ZQ, Li GS, et al. Lateral anterior approach vertebral subtotal resection fixation fusion for old osteoporotic vertebral compression fracture secondary to thoracolumbar kyphosis [J]. *Chinese Journal of Minimally Invasive Surgery*, 2021, 21(03): 220-225.
- 13) Uribe JS, Harris JE, Beckman JM, Turner AW, Mundis GM, Akbarnia BA. Finite element analysis of lordosis restoration with anterior longitudinal ligament release and lateral hyperlordotic cage placement. *Eur Spine J*. 2015 Apr; 24 Suppl 3: 420-6. DOI: 10.1007/s00586-015-3872-7. Epub 2015 Mar 13. PMID: 25772093.
- 14) Leveque JC, Yanamadala V, Buchlak QD, et al. mismatch: decreased blood loss with lateral hyperlordotic interbody grafts as compared with pedicle subtraction osteotomy. *Neurosurg Focus*. 2017 Aug; 43(2): E15. DOI: 10.3171/2017.5.FOCUS17195. PMID: 28760028.
- 15) Cho MS, Seo EM. Efficacy and radiographic analysis of oblique lumbar interbody fusion in treating lumbar degenerative spondylolisthesis with sagittal imbalance. *Neurosurg Rev*. 2021 Aug; 44(4): 2181-2189. DOI: 10.1007/s10143-020-01390-4. Epub 2020 Sep 17. PMID: 32939605.
- 16) Park SJ, Lee CS, Chung SS, et al. The Ideal Cage Position for Achieving Both Indirect Neural Decompression and Segmental Angle Restoration in Lateral Lumbar Interbody Fusion (LLIF). *Clin Spine Surg*. 2017 Jul; 30(6): E784-E790. DOI: 10.1097/BSD.0000000000000406. PMID: 27352372.
- 17) Chen E, Xu J, Yang S, et al. Cage Subsidence and Fusion Rate in Extreme Lateral Interbody Fusion with and without Fixation [J]. *World Neurosurg*, 2019, 122: e969-e977. DOI: 10.1016/j.wneu.2018.10.182.
- 18) Mobbs RJ, Phan K, Malham G, et al. Lumbar interbody fusion: techniques, indications and comparison of interbody fusion options including PLIF, TLIF, MI-TLIF, OLIF/ATP, LLIF and ALIF. *J Spine Surg*. 2015 Dec; 1(1): 2-18. DOI: 10.3978/j.issn.2414-469X.2015.10.05. PMID: 27683674; PMCID: PMC5039869.
- 19) Sembrano JN, Yson SC, Horazdovsky RD, et al. Santos ER, Polly DW Jr. Radiographic Comparison of Lateral Lumbar Interbody Fusion Versus Traditional Fusion Approaches: Analysis of Sagittal Contour Change. *Int J Spine Surg*. 2015 May 19; 9:16. DOI: 10.14444/2016. PMID: 26114085; PMCID: PMC4480050.
- 20) Tan J, Chen GP, Hao YQ. "Key technologies of biological 3D printing and advances in orthopaedic applications." *Chinese Journal of Orthopaedics*. 02 (2020): 110-111-112-113-114-115-116-117-118. doi: 10.3760/CMA.j.issn.0253-2352.2020.02.007.
- 21) Yang DP., Xia X., "3D printed biomaterials research and its clinical application advantages." *Chinese Tissue Engineering Research* 21.18 (2017): 2927-2933. DOI: CNKI:SUN:XDKF.0.2017-18-024.
- 22) Yson SC, Sembrano JN, Santos ER, et al. Repositioning before posterior fixation produces greater lordosis in lateral lumbar interbody fusion (LLIF)? *J Spinal Disord Tech*. 2014 Oct; 27(7): 364-9. DOI: 10.1097/BSD.0b013e318268007b. PMID: 22801455.
- 23) Ge TH, et al. "Effect of oblique lateral interbody fusion combined with posterior fixation for degenerative lumbar spondylolisthesis on the force lines of the operated segments." *Chinese Journal of Orthopaedics* 41.03(2021): 141-148.
- 24) Tohme AG, Khorsand D, Watson B, et al. Radiographical and clinical evaluation of extreme lateral interbody fusion: effects of cage size and instrumentation type with a minimum of 1-year follow-up. *Spine (Phila Pa 1976)*. 2014 Dec 15; 39(26): E1582-91. DOI: 10.1097/BRS.0000000000000645. PMID: 25341985.
- 25) Been E, Barah A, Marom A, et al. Vertebral bodies or discs: which contributes more to human-like lumbar-lordosis [J]. *Clin Orthop*, 2010, 468(7): 1822-1829.
- 26) Mao U, Zhao J, Dai KR, et al. Bilateral decompression using a uni-lateral pedicle construct for lumbar stenosis [J]. *Int Orthop*, 2014, 38(3): 573-57.

- 27) Obstructive Lung Disease in Children with Idiopathic Scoliosis [J]. Gary L. McPhail, Zarmina Ehsan, Sacha A. Howells, R. Paul Boesch, Matthew C. Fenchel, Rhonda Szczesniak, Viral Jain, Steven Agabegi, Peter Sturm, Eric Wall, Greg J. Redding. *The Journal of Pediatrics*. 2015(4).
- 28) Schwab F, Blondel B, Chay E, et al. The comprehensive anatomical spinal osteotomy classification [J]. *Neurosurgery*, 2014, 74(1): 112-120.
- 29) Zhao Y, Zhang M, Li Q, Chen X. Tissue Engineering Material KLD-12 Polypeptide/TGF- β 1 the Protective Effect and Mechanism of Nanofiber Gel on Early Intervertebral Disc Degeneration. *Cell Mol Biol (Noisy-le-grand)*. 2022 Mar 31; 68(3): 282-293. doi: 10.14715/cmb/2022.68.3.31. PMID: 35988181.
- 30) Tabin, S., Gupta, R., kamili, A., parray, J. Medical and medicinal importance of Rheum spp. collected from different altitudes of the Kashmir Himalayan range. *Cellular, Molecular and Biomedical Reports*, 2022; 2(3): 187-201. doi: 10.55705/cmb.2022.349901.1050
- 31) Zhang Q, Du P, Zhang Y. The effect of locating and sliding of facet combined with percutaneous endoscopic lumbar discectomy on cell inflammatory indicators and the treatment of disc herniation. *Cell Mol Biol (Noisy-le-grand)*. 2022 Feb 4; 67(5): 181-187. doi: 10.14715/cmb/2021.67.5.25. PMID: 35818255.
- 32) Du P, Zhang Q, Zhang Y. The role of IL-6, IL-10, and PGE2 in the treatment of intervertebral disc herniation by dual-channel endoscopic lumbar discectomy. *Cell Mol Biol (Noisy-le-grand)*. 2022 Feb 4; 67(5): 188-195. doi: 10.14715/cmb/2021.67.5.26. PMID: 35818254.

Fund Name:

Jilin Province health technology innovation project(No: 2019J047); "13th five year plan" science and technology project of Jilin Provincial Department of Education(No:JJKH-20180364KJ); Science and technology research project of Jilin Provincial Department of Education(No:JJKH20220074KJ).

Corresponding Author:

TIANMING GUO

Orthopaedic second treatment area, Affiliated Hospital of Beihua University, No. 13, Jiefang Middle Road, Chuanying District, Jilin, Jilin132000, China

Email: guotianming2208@163.com

(China)